Article

Direct Measurement of Water States in Cryopreserved Cells Reveals Tolerance toward Ice Crystallization

Jan Huebinger,[1] Hong-Mei Han,[1] Oliver Hofnagel,[2] Ingrid R. Vetter,[3] Philippe I. H. Bastiaens,[1] and Markus Grabenbauer[1,4,*]

[1]Department of Systemic Cell Biology, [2]Electron Microscopy Facility, and [3]Department of Mechanistic Cell Biology, Max Planck Institute of Molecular Physiology, Dortmund, Germany; and [4]Institute for Anatomy and Cell Biology, University of Heidelberg, Heidelberg, Germany

ABSTRACT Complex living systems such as mammalian cells can be arrested in a solid phase by ultrarapid cooling. This allows for precise observation of cellular structures as well as cryopreservation of cells. The state of water, the main constituent of biological samples, is crucial for the success of cryogenic applications. Water exhibits many different solid states. If it is cooled extremely rapidly, liquid water turns into amorphous ice, also called vitreous water, a glassy and amorphous solid. For cryo-preservation, the vitrification of cells is believed to be mandatory for cell survival after freezing. Intracellular ice crystallization is assumed to be lethal, but experimental data on the state of water during cryopreservation are lacking. To better understand the water conditions in cells subjected to freezing protocols, we chose to directly analyze their subcellular water states by cryo-electron microscopy and tomography, cryoelectron diffraction, and x-ray diffraction both in the cryofixed state and after warming to different temperatures. By correlating the survival rates of cells with their respective water states during cryopreservation, we found that survival is less dependent on ice-crystal formation than expected. Using high-resolution cryo-imaging, we were able to directly show that cells tolerate crystallization of extra- and intracellular water. However, if warming is too slow, many small ice crystals will recrystallize into fewer but bigger crystals, which is lethal. The applied cryoprotective agents determine which crystal size is tolerable. This suggests that cryoprotectants can act by inhibiting crystallization or recrystallization, but they also increase the tolerance toward ice-crystal growth.

INTRODUCTION

Freezing of mammalian cells is usually lethal if no precautions are taken. However, cryopreservation or cryoconservation techniques have been developed that enable the reversible arrest of life in structurally intact cells and tissues by freezing (1). Despite the broad applications of cryogenic storage in biomedical research and reproductive medicine, the underlying mechanisms are poorly understood and progress is often achieved empirically.

The physical state of water, the most abundant substance in living matter, is considered a key factor for successful cryopreservation. Solidified water exhibits interesting anomalies, emerging in 16 known ice-crystal structures (more than for any other substance) and several amorphous solid states (2–4). When cooled at ambient pressure, water can crystallize to hexagonal or cubic ice depending on the cooling rate. Yet, if aqueous solutions are cooled extremely rapidly, any crystallization is avoided and the water becomes vitrified, resulting in what is sometimes called vitreous water or vitreous ice, a glassy and amorphous solid (for review, see Dubochet (5)). This is the preferred condition for investigating biological material by cryoelectron microscopy (cryo-EM).

During freezing for cryopreservation, one tries to avoid the main causes of cell death, which are assumed to be intracellular ice-crystal formation (6,7) and lethal concentrations of solutes (8,9). The suppression of ice crystallization is achieved by two different approaches: 1) slow cooling associated with a massive dehydration of cells, and 2) rapid cooling (also known as vitrification) (1,10–13). After both of these approaches, the cells themselves are assumed to be in an ice-crystal-free, vitrified state (1,10–12). It has been suggested that small intracellular ice crystals might be tolerable, but the extent of this tolerability remains unclear and experimental evidence is lacking (for review, see Wowk (11)). Most authors have stated that the avoidance of intracellular ice crystallization is the key to cell survival (11,13,14). Currently, all cryopreservation procedures rely on the application of cryoprotective agents (CPAs), which aim to prevent ice-crystal formation.

However, cryogenic arrest is also used to investigate cells in a close-to-native state by cryo-EM, the method of choice for determining cellular ultrastructure at the highest possible resolution (5). For such sample preparation, the immediate arrest of molecules is best achieved by high cooling rates through rapid cryofixation, transforming water into vitreous water. Insufficient cooling rates result in the emergence of

Submitted May 5, 2015, and accepted for publication September 23, 2015.

*Correspondence: grabenbauer@uni-heidelberg.de

Editor: Andreas Engel.

0006-3495/16/02/0840/10

http://dx.doi.org/10.1016/j.bpj.2015.09.029

ice crystals with either a hexagonal or cubic configuration. Generally, the formation of crystalline ice needs to be strictly avoided, as cellular and molecular components might be artificially displaced and perturbed (5,15). Cryo-EM allows for the direct and precise determination of different states of water and their localization at high resolution by cryoelectron diffraction (15). We find that mammalian cells that have been vitrified for EM and shown to be in a native state with intact cellular structures do not survive after subsequent warming to physiological temperatures. However, this apparent paradox may be explained by ice-crystal formation during warming.

Below the so-called vitrification temperature of approximately –130°C, crystallization does not occur. However, during cooling as well as during warming, an aqueous sample has to traverse the temperature range of ice-crystal nucleation and formation, typically between 0°C and –130°C. As fewer and larger ice crystals are energetically favorable over multiple small ones, the ice will recrystallize to fewer but larger ice crystals with time. If this lethal zone is crossed fast enough during rapid freezing and warming, ice crystals cannot form or grow at all. But there is a specific problem inherent in the warming back up of cryopreserved samples, because the warming and cooling rates decrease when the final temperatures are approached (Fig. 1).

This delay is not due to a specific property of the sample, but rather is governed by Fourier's law of heat conduction:

$$q = \kappa(\Delta T/L). \quad (1)$$

Here, the heat flux (q) is proportional to the thermal conductivity (κ) and the difference in temperature (ΔT) divided by the distance to the surface (L). If ΔT decreases, the heat flux will always decrease. Since mammalian cells are very sensitive to overheating, they cannot be warmed much higher than their physiological temperature (37°C). This upper limit renders the warming process much more difficult than cooling.

Investigating the water state of samples during the whole procedure of cryopreservation is difficult. Usually, differential scanning calorimetry (DSC) is used to measure the exothermic events of ice crystallization and recrystallization upon slow warming (16–19). Therefore, the water states during a fast warming process cannot be monitored. As an indirect measurement, DSC is neither used quantitatively nor applied directly to the cryopreserved sample itself. Instead, it is mainly used on cell-free medium samples to analyze the freezing properties of different cryoprotectants.

In this study, we directly measured the states of water at low temperatures inside cryopreserved cells by cryo-EM/electron diffraction and x-ray diffraction. We focused on rapid-freezing protocols, as the slow-freezing mechanisms in cryopreservation are rather established and are accompanied by massive dehydration that cannot be tolerated by all

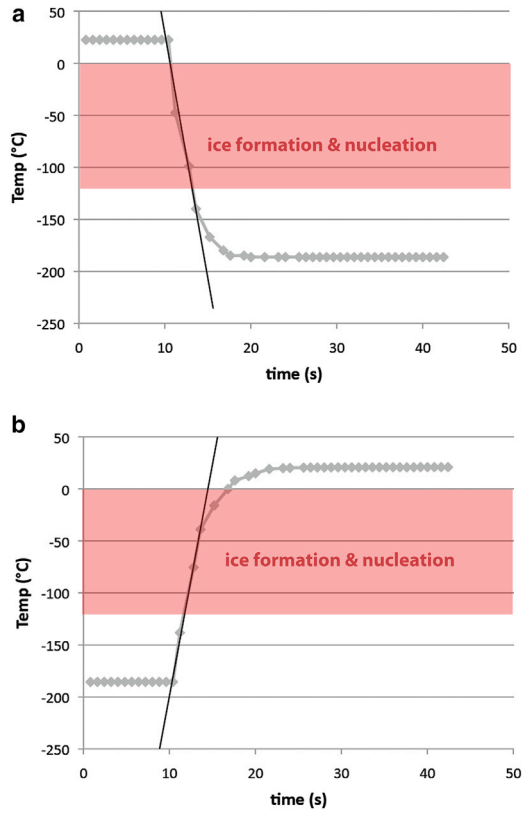

FIGURE 1 Typical cooling and warming curve. (*a* and *b*) Temperature traces of an insulated thermocouple (*gray*) that was first plunged into liquid nitrogen (*a*) and then warmed in a water bath (*b*) are shown, resembling a typical fast-freezing protocol for cryopreservation. The initial rates are comparable (*black lines*: –47°C/s (*a*) and +44°C/s (*b*)), but due to slowing down in the final phase of warming, the sample takes nearly three times longer to traverse the critical temperature range in which ice crystals can be formed (*red area*: 2.6 s (*a*) and 7.3 s (*b*)).

cell types and most tissues (7,13). Our analysis of water phases at high spatial resolution allowed us to differentiate between extra- and intracellular areas. By correlating the water phases of cryopreserved samples with cell survival, we found that extracellular ice formation takes place in established cryopreservation protocols—including those that involve rapid cooling—without affecting subsequent cell survival. Furthermore, by warming vitrified cell samples to different temperatures, we found that the cells could also tolerate massive intracellular ice crystallization. Only when the samples were warmed even further and many small ice crystals recrystallized into fewer but larger crystals did cell survival decrease. The tolerance level of intracellular ice recrystallization was strongly determined by the applied cryoprotectants. This implies that cryoprotectants do not act solely as inhibitors of ice crystallization. They seem to be even more efficient at inhibiting recrystallization. Further, certain cryoprotectants also lead to cellular tolerance of recrystallization. Based on these (to our knowledge) novel findings regarding the mechanisms of cell survival, new cryopreservation protocols and types of

cryoprotectants can be designed to preserve more (if not most) cell and tissue types for biomedical research.

MATERIALS AND METHODS

Cell culture

Cell cultures were prepared as described previously (20). Briefly, HeLa cells (ATCC No. CCL-185) were grown at 37°C with 5% CO_2 in Dulbecco's modified Eagle's medium supplemented with 10% fetal calf serum, 2 mM L-glutamine, and 1% nonessential amino acids.

Composition of the cryoprotective media

EAFS (ethylene glycol, acetamide, Ficoll, and sucrose), which was originally developed for cryopreservation of oocytes, was prepared as described previously (17,18,21). Briefly, 10% ethylene glycol (Serva, Heidelberg, Germany) and 10.7% acetamide (Acros Organics, Geel, Belgium) were dissolved in 30% (w/v) Ficoll PM 70 (GE Healthcare, München, Germany) and 0.5 M sucrose (Serva, Heidelberg, Germany) in PB1 medium. PB1 medium is phosphate-buffered saline (PBS) medium supplemented with 3 g/L bovine serum albumin, 1 g/L glucose, and 0.036 g/L sodium pyruvate.

DES medium is used for cryopreservation by vitrification (22–27). Hence, 15% dimethyl sulfoxide (DMSO), 15% ethylene glycol, and 0.5 M sucrose (all from Serva, Heidelberg, Germany) were mixed in PBS containing 20% fetal calf serum. DE medium was prepared accordingly, but without the addition of sucrose.

In cryofixation for cryo-EM of vitrified sections (CEMOVIS), dextran is frequently used as a cryoprotectant, usually in concentrations of 20–30% (w/v) (20,28). We prepared dextran with an average molecular mass of 40 kDa (Sigma-Aldrich, Taufkirchen, Germany) as a 30% solution in PBS.

Plunge freezing of cells

HeLa cells were grown on glow-discharged gold EM grids (300 mesh) covered with a Quantifoil R2/4 film (PLANO, Wetzlar, Germany) in 35 mm petri dishes (Greiner Bio-One, Frickenhausen, Germany). After ~6 h, adherence of the cells was confirmed microscopically. The grids were then washed in PBS, incubated with the particular cryoprotectant, blotted, and plunged in liquid ethane at –170°C using a CP3 plunge freezer with a controlled humidity chamber (Gatan, Munich, Germany). The different cryoprotectants were pipetted on the grid (4 μL) immediately before the sample was mounted in the plunge freezer, and excess medium was blotted away from the back side of the grid using filter paper (Whatman No. 4; Whatman, Datteln, Germany). The blotting and mounting took at least 40 s, ensuring complete penetration of cell-permeable cryoprotectants into the cells. The blotting times were carefully adjusted to obtain a very thin film of medium while avoiding drying of the sample (8 s for PBS, 12 s for DE, and 25 s for the highly viscous dextran and EAFS solutions).

Self-pressurized rapid freezing

Self-pressurized rapid freezing (SPRF) was introduced as an alternative cryofixation method that included subsequent freeze substitution and resin embedding for room-temperature EM (34). An improved protocol to achieve vitrification of biological samples after SPRF using dextran was reported recently (35,36). Briefly, cell suspensions with 2.5×10^7 cells/mL were prepared using different cryoprotective media and taken up into biocompatible aluminum tubes (300 μm inner diameter and 600 μm outer diameter; Goodfellow, Bad Nauheim, Germany) (35). First, aluminum tubes were inserted into a disposable pipette tip mounted on a 0.5–10 μL micropipette. Next, the micropipette volume was set to 3–4 μL in excess of the tube capacity (~1 μL) to allow for overfilling of the capillary. Then the open end of the capillary was inserted into the specimen suspension and the fluid was drawn into the tube very carefully to prevent formation of internal air bubbles. The tubes were then sealed at both ends by means of flat-jawed pliers. The closed tubes were plunged horizontally into liquid ethane cooled by liquid nitrogen using an in-house-made plunge freezer.

Temperature treatments

Plunge-frozen grids were taken from liquid-nitrogen storage and warmed in an automated freeze-substitution device (AFS2; Leica Microsystems, Vienna, Austria) to the adjusted maximum temperatures (specified in the corresponding experiments) for 30 s. They were then placed on a precooled metal surface and transferred back into liquid nitrogen for subsequent cryo-EM examination or thawing, followed by survival tests (see Fig. 4 *b*).

SPRF tubes were warmed for 30 s in a cryostage set between –140°C and –20°C (THMS 600; Linkam Scientific Instruments, Tadworth, UK) by putting them directly on the silver block of the stage, and thawed directly in a 37°C water bath for subsequent cell survival tests. The cryostage can be used for this purpose because the flow of nitrogen that protects the sample from humidity in the AFS is not necessary in this case. Due to its small size, the cryostage can be placed between the liquid nitrogen and water bath to avoid any temperature equilibration during transfer.

Cell viability tests

Cells grown on grids were transferred directly from liquid nitrogen into 24-well plates containing 2 mL of prewarmed cell culture medium at 37°C and cultured overnight at 37°C and 5% CO_2. The medium was then replaced by a propidium iodide solution (12 μg/mL in PBS) to label dead cells. The grids were imaged on a Zeiss Axiovert microscope with a 10× objective (Carl Zeiss AG, Oberkochen, Germany).

After SPRF, cell viability was quantified as the recultivatable proportion of cells. Thawed tubes were cut open on one end (the filled tubes could be cut with ordinary scissors without collapsing). Subsequently, they were mounted on a pipette tip (0.1–10 μL) with the closed end sticking out of the tip. The closed end was cut open and the solution was pipetted into 200 μL of cell culture medium in an eight-well glass-bottom cell culture dish (Thermo Fisher Scientific, Rochester, NY). The cells were cultured at 37°C and 5% CO_2, and adherence was quantified after 4 h. The cell concentration in the supernatant was determined using a hemocytometer. The cells were then washed, trypsinized, and taken up in 200 μL solution to determine the concentration of adherent cells.

Cryo-EM and tomography

Samples were transferred into a JEM-3200 FSC electron microscope (JEOL Germany, Eching, Germany) equipped with an 8K×8K TemCam-F816 CMOS camera (TVIPS, Gauting, Germany) and analyzed at liquid-nitrogen temperature. The accelerating voltage was set to 200 kV and an energy filter at zero-loss filtering was used to enhance contrast. Ice thickness was measured with the help of an energy filter as previously described (37). Areas that were >100 nm thick (including the Quantifoil film) were selected. Overview images were taken at 9000× magnification and the ice state of selected areas was determined by electron diffraction.

For tomography, tilt series from –60° to approximately +60° were recorded at 19,000× magnification in 2° increments using EM Tools software (TVIPS, Gauting, Germany). Stacks were mounted, aligned, and reconstructed with the use of IMOD software (38,39). Side views of the tomograms were created with the UCSF Chimera package (40).

Cell volume measurement

Cells transfected with soluble enhanced green fluorescent protein (EGFP)-protein (pEGFP-N1; Takara Bio Europe/Clontech, Saint-Germain-en-Laye, France) were analyzed to measure relative cell volumes using a 60× 1.4 NA oil-immersion objective on a confocal fluorescence microscope at 488 nm excitation (Leica TCS SP5; Leica Microsystems CMS, Mannheim, Germany). During recording, the cell culture medium was exchanged with test medium using an in-house-made pumping system with temperature control (Prof. F. Wehner, MPI Dortmund). Image analysis was done with ImageJ (National Institutes of Health, Bethesda, MD). Mean fluorescence intensity was measured using a mask around the visible intersection of the cell. An intensity increase represents cell shrinkage, as fluorescent EGFP is concentrated in the confocal volume.

X-ray diffraction

The medium was frozen in the tip of an open pulled straw (OPS) device (Vajta Embryology Consulting, RVT, Cairns, Australia) and mounted under liquid nitrogen into the beamline of a Rigaku Micro-Max-007 HF (Rigaku Europe SE, Ettlingen, Germany). X-ray diffractograms were collected at the Cu k-α wavelength within a stream of cold nitrogen at –173°C using a MAR345dtb image plate detector (MAR research, Hamburg, Germany).

RESULTS

For high-resolution imaging by cryo-EM, cells are usually cryofixed by plunge freezing, high-pressure freezing, or the recently developed SPRF method. The latter two methods are used for thicker samples and vitrification is achieved with the help of CPAs, typically dextran. Vitrification of the cells is proven directly and unambiguously on the sample by electron diffraction (15,28,35). Yet, when we warmed dextran-cryoprotected samples relatively fast in a water bath or prewarmed culture medium, all of the cells died (Fig. 2 *a*), even though the treatment before cooling is not harmful (35). This indicates that vitrification alone is not sufficient for cryopreservation.

However, to ensure cell survival during cryopreservation, different CPAs are used. Such CPAs are typically found empirically and the question arises as to how they preserve cells. Therefore, we chose two typical CPA combinations used in cryopreservation: EAFS (composed of cell-permeable ethylene glycol and acetamide, and the nonpermeable components Ficoll and sucrose) and DES (cell-permeable DMSO and ethylene glycol and nonpermeable sucrose). Both showed high survival rates after freezing and subsequent thawing (Fig. 2 *a* and Fig. S1 in the Supporting Material). The extracellular compounds caused cell shrinkage, which was monitored by the intracellular fluorescence increase (Fig. 2 *b*). Hence, to distinguish cell shrinkage from genuine ice formation effects, we designed a CPA medium that avoids a cell volume decrease. This DE medium (DMSO and ethylene glycol) also showed high cell survival after freezing/thawing (Fig. 2 *a*).

To investigate which water phases are obtained in cryopreservation using established CPAs, we froze samples in OPSs, which are rather established cryopreservation tools

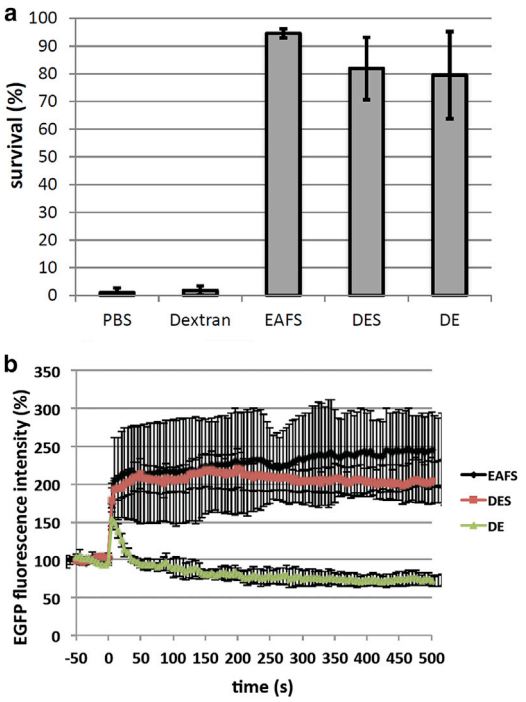

FIGURE 2 Effects of cryoprotective media on survival rates and cell volumes. (*a*) Survival rates in different media were assessed by reculturing cells after SPRF and subsequent fast warming. (*b*) Confocal slices in cells transfected with soluble EGFP were imaged over time. At time point 0, the medium is exchanged to the indicated cryoprotective media. The mean fluorescence intensity increase shows a decrease in volume.

(41). We tested five different cryoprotective media (EAFS, DES, 100% DE, 60% DE, and 20% DE) by x-ray diffraction after freezing in OPSs and correlated the corresponding survival rates (Fig. 3). As a negative control, PBS showed mainly hexagonal ice without any cell survival. EAFS showed clearly vitrified water; DES formed mainly cubic ice, a small part of which was vitrified at the tip; 100% DE crystallized to cubic ice; and 60% and 20% DE gave rise to hexagonal ice. In correlation with the survival rates after these treatments, the results clearly show that crystalline ice emerges during cooling when established cryopreservation protocols designed for vitrification are used. Nevertheless, in certain conditions, such massive ice crystallization is tolerated and high survival rates can still be achieved.

This shows that vitrification of the medium is not necessary for successful cryopreservation by fast freezing. However, since the enclosed cells have a relatively small volume compared with the extracellular medium in this approach, the contribution of the intracellular region to the overall signal is small. Therefore, a possible scenario is that the extracellular medium is crystallized and only the cell interior is vitrified.

To distinguish intra- and extracellular water phases and correlate them with cell survival, we designed a special protocol. Cells that were grown on EM grids and directly cryofixed by plunge freezing in liquid ethane (–170°C)

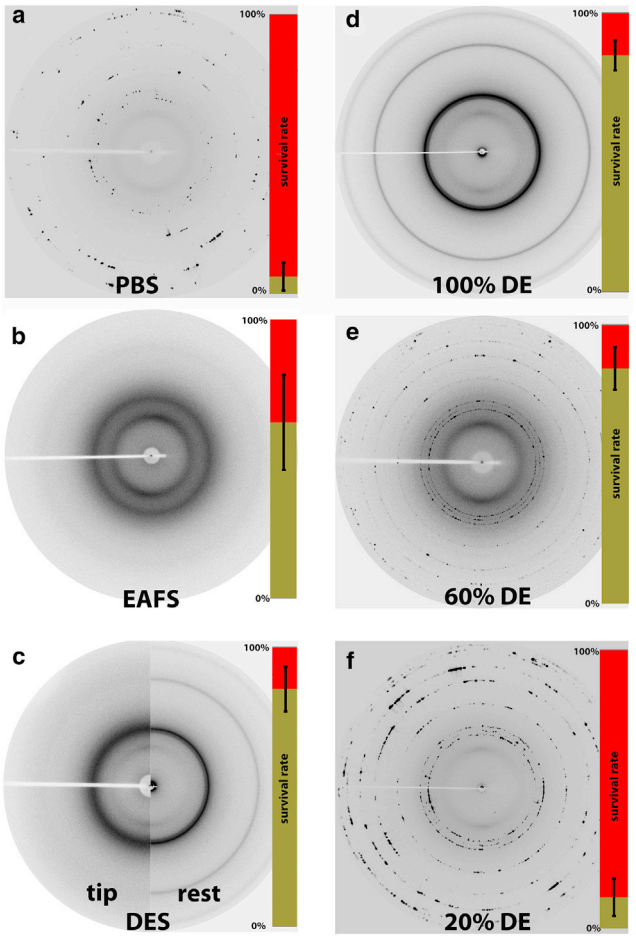

FIGURE 3 X-ray diffraction of different media frozen in OPS. The media were frozen in the tip of the OPS and analyzed by x-ray diffraction. The corresponding survival rates of HeLa cells are shown in insets. (*a*) PBS. (*b*) EAFS. (*c*) DES. (*d*) 100% DE. (*e*) 60% DE. (*f*) 20% DE medium. (*a*), (*e*), and (*f*) show typical diffraction patterns of hexagonal ice. (*c*) (*right half*) and (*d*) show typical patterns generated by cubic ice. (*b*) and (*c*) (*left half*) show patterns of vitrified ice. $N = 8$; error bars represent standard deviations.

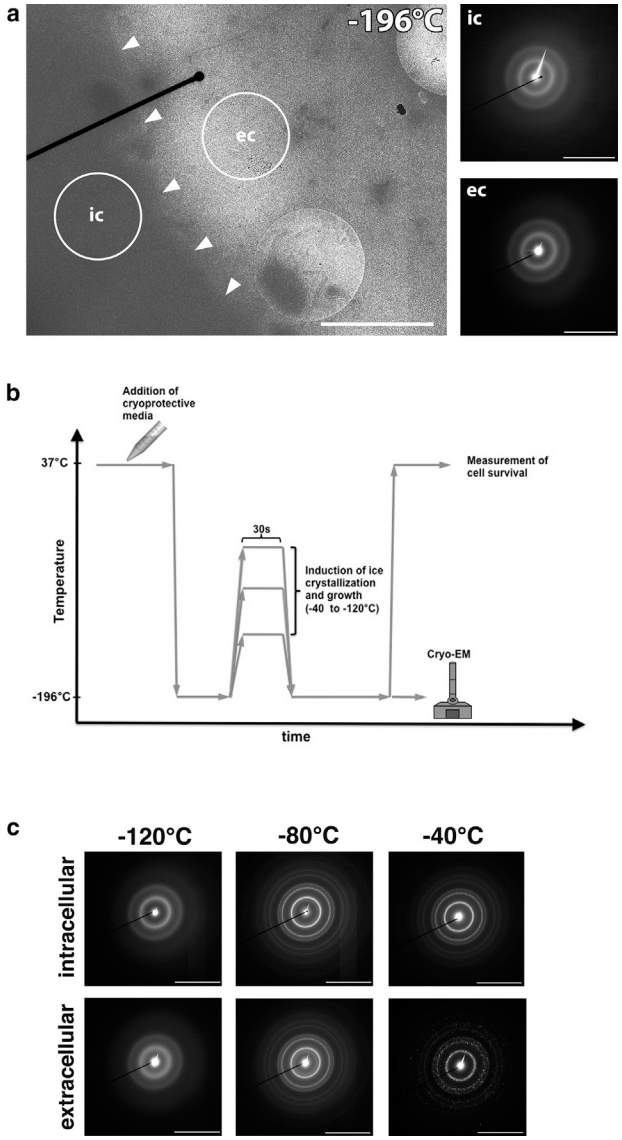

FIGURE 4 Visualization of ice crystallization in vitrified cells during warming. (*a*) HeLa cells were plunge frozen and examined by cryo-EM. The water states of the indicated areas (ic, intracellular; ec, extracellular) were analyzed by electron diffraction. Arrowheads mark the cell edge. (*b*) Schematic view illustrating the procedure used to induce ice-crystal formation during warming. The cell culture medium is replaced by test medium and the cells are frozen by plunging in liquid ethane and kept in liquid nitrogen. After warming to the indicated temperatures for 30 s, the cells are transferred back to liquid nitrogen and either imaged by cryo-EM at –196°C or thawed rapidly for subsequent analysis of survival rates. (*c*) Diffractograms of cells subjected to the protocol shown in (*b*). Maximum warming temperatures are indicated. Blurred rings represent a completely vitrified sample. Sharp rings after warming to –80°C and spotted rings at –40°C represent crystalline ice, with the latter containing less (but potentially larger) crystals. Images are representative of at least 15 cells from at least three different freezing experiments. Scale bars: 2 μm for micrographs, 1/0.11 nm for diffractograms.

exhibited flat parts that were accessible to cryo-EM analysis. By electron diffraction at –196°C, the water phases could be determined and assigned to intra- and extracellular areas. Without the addition of CPAs, we found solely cells showing two blurred rings in the diffractograms (Fig. 4 *a*) that represent vitrified water (15). Vitrified water is metastable and does not crystallize below the so-called vitrification temperature of approximately –130°C, as the energy in the system is too low. To visualize the process of ice-crystal nucleation and growth during warming, we designed an experimental sequence as shown in Fig. 4 *b*. Cells were subjected to different types of CPAs, cryofixed, and kept at –196°C. The samples were then warmed to a maximum of –120°C, –80°C, or –40°C, respectively, left for 30 s at these temperatures, and cooled down to –196°C again. At these higher temperatures and ambient pressure, hexagonal ice is the stable form of water, and the energy is high enough for it to crystallize over time. As fewer large ice crystals are energetically favorable over many smaller ones, ice will recrystallize to fewer but larger crystals with time. Ice

crystals that emerge at these higher temperatures keep their shape, size, and crystal lattice during recooling at ambient pressure and therefore are accessible for structural analysis by cryo-EM and electron diffraction. Using this procedure, we could show that samples that were warmed to –120°C for 30 s remained vitrified even when they were frozen without CPAs (Fig. 4 *c*). When the samples were warmed to –80°C for 30 s, extra- and intracellular parts of the samples completely crystallized, mirrored in sharp rings in the cyo-electron diffractogram. When warmed to –40°C, the crystals grew larger and were already detectable in the imaging mode of the cryoelectron microscope. The sharp rings in the diffractogram became spotted, reflecting a lower number of larger hexagonal ice crystals in the selected area (Fig. 4 *c*). Since the samples were vitrified initially, all crystallization and recrystallization must have occurred during warming.

To investigate whether intra- and/or extracellular ice crystallization can be tolerated during cell survival, we tested different CPAs by applying the above-described experimental setup (Fig. 5) and correlated them with survival rates obtained using the same temperature treatments (Fig. 6). Using EAFS, DES, or DE medium as cryoprotectants in our warming procedure (Fig. 5 *b*), we found that the sample remained completely vitrified after cells were warmed to –120°C for 30 s (Fig. 5, *a–c*), and survival was not impaired (Fig. 6). For EAFS and DES medium, cells could also be warmed up shortly to –60°C without any negative consequences for survival. However, warming to –40°C or any higher temperature was absolutely lethal and was associated with a prominent occurrence of hexagonal ice in the electron diffractograms (Fig. 5, *a* and *b*). In contrast, the survival rate of cells treated with the nonshrinking DE medium decreased gradually at each temperature step above –120°C, with some cells even surviving a maximum warming up to –20°C.

When we correlated cell survival rates with the occurrence of ice crystals as observed by cryo-EM, we found vitreous water in the EAFS medium in intra- and extracellular areas after warming up to –80°C. Some spots of hexagonal ice in electron diffractograms (Fig. 5 *a*), which were also visible as electron-dense crystals in microscopic imaging mode, were grown outside cells, as visualized in 3D by cyo-electron tomography (see Fig. S2 and Movie S1). DES medium samples turned completely crystalline (cubic ice) under these conditions, but survival was not impaired (Figs. 5 *b* and 6). Such massive water crystallization to cubic

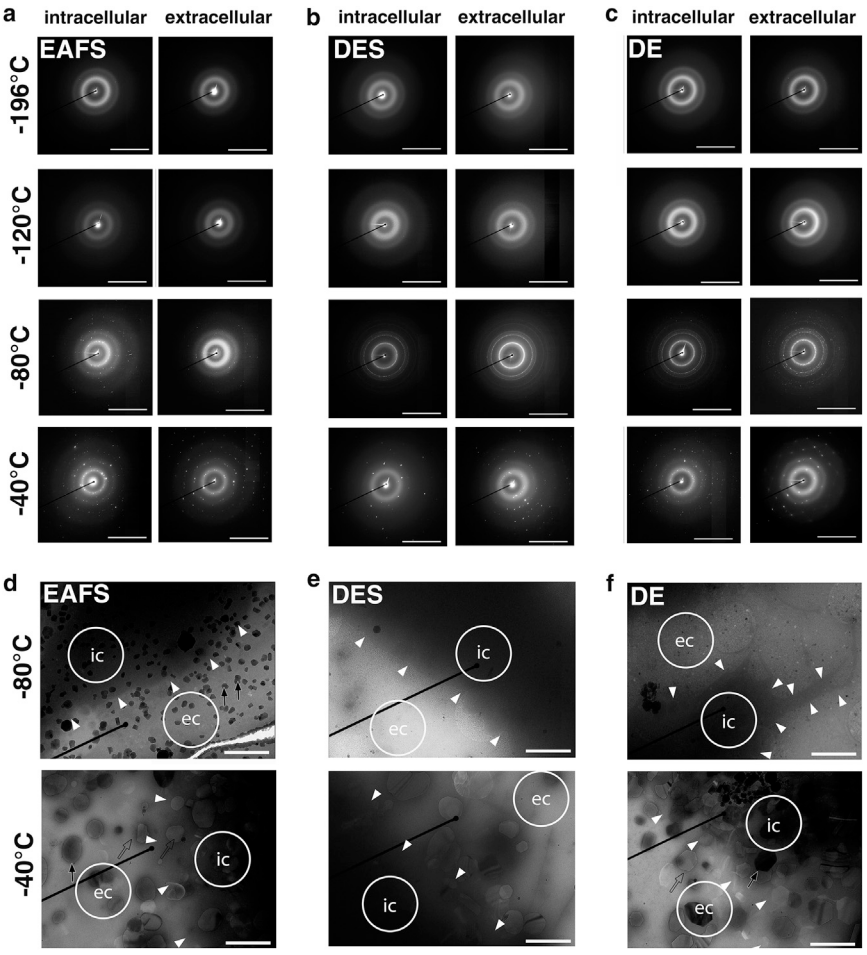

FIGURE 5 Cryo-EM of cryoprotected HeLa cells at different temperatures. Cryoelectron diffractograms and micrographs were obtained from cells treated as described in Fig. 4 *b*. The diffractograms show intra- and extracellular areas of the sample. (*a*) Cells incubated in EAFS show a transition from vitreous water at –196°C and –120°C to hexagonal ice crystals at –40°C. (*b* and *c*) In DES and DE medium, the crystallization of ice occurs below –80°C in intra- and extracellular parts simultaneously. (*d*) Ice crystals at –80°C in EAFS medium are electron dense and outside cells (see Fig. S2). (*e* and *f*) The ice crystals in DES and DE medium at –80°C are homogeneously distributed. At –40°C, all samples contain large intra- and extracellular ice crystals embedded in vitrified water. Circles indicate the areas of diffractograms (ic, intracellular; ec, extracellular). White arrowheads point to the border of the cells. Some crystals show higher electron density (*solid black arrows*) than others (*open black arrows*). Images are representative of at least 15 cells from at least three different freezing experiments. Scale bars: 2 μm for transmission EM, 1/0.11 nm for diffractograms.

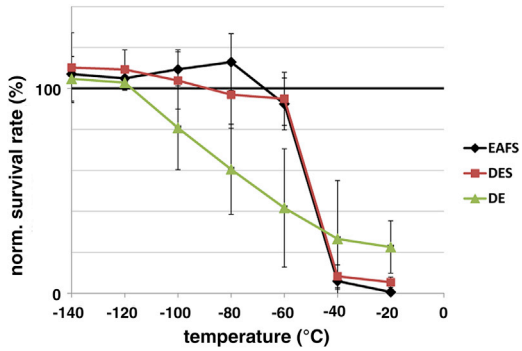

FIGURE 6 Correlation of temperature treatment with subsequent cell survival. Cells were cryofixed in EAFS (*black*), DES (*red*), or DE medium (*green*). After warming to the indicated temperatures for 30 s and subsequent rapid thawing, survival rates were determined. Error bars represent standard deviations.

ice seems nonhazardous to cells. Samples warmed to −40°C yielded electron-dense crystals, as was observed during warming to –80°C in EAFS, but additionally contained another population of hexagonal crystals inside the sample (Fig. 5, *a* and *d*). These crystals were localized within the sample plane in extra- and intracellular areas, as revealed by the 3D analysis (Movie S2), and most likely are responsible for the lethal effect.

Samples cryoprotected by nonshrinking DE medium were completely crystallized after warming to –80°C, without any detectable fraction of vitreous water (Fig. 5 *c*). Small hexagonal ice crystals were evenly distributed inside and outside the biological material. Warming to a maximum of –40°C caused severe ice-crystal growth (Fig. 5 *f*). Since survival was reduced but still present in both conditions, it appears that the occurrence of intracellular hexagonal ice crystals is not lethal, whereas survival decreases with crystal growth.

The tolerable crystal sizes depend specifically on the chosen cryoprotective medium. In DE medium, cells survived intracellular ice crystals with an average length of 1–3 μm, whereas in EAFS medium, even 0.4–0.8 μm crystals were lethal (see Fig. S3).

DISCUSSION

Cryopreservation (i.e., the reversible arrest of cells or tissues) can be achieved by fast freezing. The general assumption is that proper vitrification of the sample is the critical step to achieve survival, as delineated in recent literature (1,11,13,42). Although some investigators have speculated that certain amounts of intracellular ice crystals may be harmless (12), experimental proof has been lacking. Here, using cryo-EM and x-ray diffraction, we have shown that ice crystals occur during conventional cryopreservation in both extra- and intracellular areas of living cells. Recently, Paredes and Mazur (43) showed that the vitrification of external medium has little or no correlation to cell survival. However, the authors' conclusions were based on freezing cell-free media and they did not directly determine the water/ice phases. More surprising was our finding that even intracellular water crystallization can be tolerated and survived by cells.

Remarkably, mammalian cells that are perfectly vitrified for cryo-EM analysis, typically with dextran used as the cryoprotectant, do not survive after warming. Of course, one could speculate that ice formation during the thawing process is lethal, but this is not mandatory, as we showed that cells frozen in DE medium could survive intracellular ice-crystal formation during freezing. Hence, vitrification does not seem to be the sole important parameter for investigating cell survival after fast freezing. Recent studies on functional cryopreservation mainly considered the process of freezing and vitrification of biological materials (1,11,13,42). Our study shows experimentally that harmful processes take place during warming, which is supported by recent descriptive studies on the importance of high warming rates for cell survival (17,18). Due to the upper temperature limit of mammalian cells, it is more challenging to reach high warming rates than high cooling rates, and this is especially true for the temperature range directly below the melting temperature (see Fig. 1). In this phase, the recrystallization of water into fewer but larger ice crystals occurs, and ice growth and recrystallization occur most rapidly just before the melting point is reached (12,13). A recent review article noted that "it has been apparent for some time that strict avoidance of devitrification is not necessary," and concluded that recrystallization might kill cells (12). However, experimental evidence was lacking until we correlated intracellular ice-crystal size with cell lethality, providing a direct relationship between lethality and recrystallization rather than ice crystallization.

Critical factors in cell survival are the CPAs used. Currently, the application of CPAs is mandatory, as cryopreservation of mammalian cells or tissues without CPAs has not yet been achieved. It is generally assumed that CPAs mainly function in suppressing intracellular ice-crystal formation (1,11,18). However, we found that vitrification is not the sole parameter. There was a strong correlation between ice-crystal size and cell lethality for every CPA tested. Macromolecular compounds such as dextran and Ficoll are particular efficient at raising the viscosities of aqueous solutions (Table 1) and aid in the vitrification of such solutions. Therefore, one could speculate that higher viscosities delay both crystallization and recrystallization (44,45), thereby protecting cells during cryopreservation. Yet, this relationship is very inconsistent, as the most viscous CPAs tested—dextran and EAFS (see Table 1)—showed the highest and lowest survival rates, respectively (see Fig. 2 *a*). Further, the intracellular viscosity will increase dramatically upon cell shrinkage. Consequently, although the modified DE cryoprotectant mixture of DMSO and ethylene glycol, which has low viscosity and

TABLE 1 CPAs and their characteristics

CPA	Molecular Mass (g/mol)	Molecular Structure	Cell Permeable	Final Concentrations Used in This Study (%)	Viscosity in Aqueous Solution at 25°C (mPa*s)[a]
Dextran 40	40,000	branched glucose polymer	no	30 (w/v)	≈50 (29)
Ficoll 70	70,000	branched saccharose-epichlorohydrin-copolymer	no	24 (w/v)	>10[b]
Sucrose	342	glucose-fructose disaccharide	no	13–17 (w/v)	≈1.5 (30)
DMSO	78	dimethyl sulfoxide	yes	15 (v/v)	<1.5 (31)
Ethylene glycol	62	ethane-1,2-diol	yes	10–15 (v/v)	<1.5 (32)
Acetamide	59	acetamide	yes	10.7 (w/v)	<1.1 (33)

[a]Viscosity of an aqueous solution at room temperature containing single CPAs in their final concentration.
[b]Information provided by the manufacturer.

keeps cell volumes constant, should be a poor cell protectant, it provided high survival rates. Even though there is lack of experimental data for intracellular viscosities in different CPA mixtures at different temperatures, a correlation between viscosities and survival seems very unlikely. In any case, this cannot be the sole parameter, since the tolerable ice-crystal size differed significantly among different CPAs, implying a mechanism of ice crystal tolerance rather than inhibition of crystallization or recrystallization. In particular, the DE medium yielded very interesting results. This medium penetrates into cells and keeps their volume constant. Cell survival decreased gradually with increasing ice-crystal size over a broad temperature range, but without complete lethality even under the harshest conditions tested, creating larger intracellular ice crystals than the EAFS medium under lethal conditions. This implies that intracellular CPAs such as DMSO and ethylene glycol have protective effects at high concentrations that allow the cells to survive relatively large ice crystals. In addition to effects that simply inhibit ice crystallization, the cryoprotective effects of specific CPAs that lead to intracellular ice-crystal tolerance should be investigated further. The current understanding of these mechanisms at the subcellular or molecular level is still poor.

But why is recrystallization during warming more harmful to cells than the initial ice crystallization that occurs during freezing? One theory is that growing ice crystals damage cellular membranes and thereby cause lethality. However, it was pointed out that due to the hydrophobicity of the membrane plane, the model of an ice crystal piercing into membranes is not realistic (46). Moreover, based on the survival of extremely deformed, shrunken, and dehydrated cells during cryopreservation by slow freezing, one can conclude that the overall preservation of cellular structures is quite unrelated to the survival of cells (1,13,14). However, volume changes that occur upon freezing and thawing of water, leading to indirect mechanical stress on cellular membranes that are permanent in a solid phase and relatively rigid at subzero temperatures (47,48), could be potentially lethal for cells. In addition to mechanical damage by intracellular ice crystallization, high intracellular solute concentrations are also supposed to cause lethality in cryopreservation (6–8,13,46). Simply put, the more water is bound in ice crystals, the higher will be the solute concentration. During slow warming of a vitrified specimen, directly after the initial crystallization, all available (free) water crystallizes and we cannot detect a vitrified/liquid phase. The warmer the specimen gets, the more crystallized water melts into liquid phase and consequently decreases the solute concentration (13). Nevertheless, in our experimental setup, we see a massive decrease in survival after prewarming to higher subzero temperatures (e.g., –40°C for DES medium) and not upon initial crystallization, which apparently contradicts the theory of freezing damage caused by high solute concentrations. However, at higher temperatures, when molecules become more mobile, elevated solute concentrations would probably be more destructive. Further investigations will be required to determine the exact damaging mechanisms that occur during recrystallization.

Taken together, these results indicate that the detrimental effects of freezing of life can be counteracted in three ways. The first is to prevent (intracellular) ice crystallization. This is best achieved by optimizing the combination of cooling speed, warming speed, and specific CPAs, and this approach has already led to some success in cryopreservation (11,13). However, since many cell types and tissues failed to be preserved by these methods, researchers need to carefully investigate the underlying principles to find alternative methods. Our results allow for a different approach, since they imply that the ability of CPAs to inhibit recrystallization is more important than their ability to facilitate vitrification. Ice-binding proteins or substances that suppress ice-crystal growth are already promising as novel cryoprotectants (49–52). Based on our findings, they should be of great interest for fast-freezing cryopreservation, as they inhibit recrystallization to larger ice crystals.

Second, the warming protocols can be improved. Our results indicate that instead of considering just general warming speed during thawing, one should adapt warming protocols optimized for the specific cryoprotective medium used. For example, for EAFS and DES medium, the warming rates could be kept moderate between –196°C and –60°C, since within 30 s this temperature is not lethal. Warming rates above –60°C should be accelerated rapidly

for efficient cryopreservation. In DE medium, warming rates need to accelerate above –120°C, but suboptimal warming rates are better tolerated in DE than in EAFS or DES medium.

The third approach is to further investigate the mechanism that leads to tolerance of ice-crystal growth. One possibility is a modified phase change of cellular membranes during cooling in the presence of DMSO (47,48), which would probably reduce the susceptibility for mechanical damage by ice-crystal growth. On the other hand, modifications to the hydration shell of proteins or membranes might contribute to cryoprotective mechanisms. The findings presented here might enable a systematic search for new CPAs based on their ability to stabilize cellular constituents such as membranes or proteins against the detrimental action of ice-crystal growth, rather than their ability to inhibit ice-crystal formation.

In summary, the surprising results of this study regarding the state of water during freezing, storage, and warming of biological samples shed, to our knowledge, new light on the general mechanisms of cryopreservation. We believe this will help in future efforts to conserve more (if not most) of the important cell and tissue types for biomedical applications.

SUPPORTING MATERIAL

Three figures and two movies are available at http://www.biophysj.org/biophysj/supplemental/S0006-3495(15)01000-0.

AUTHOR CONTRIBUTIONS

J.H.: acquisition, analysis, and interpretation of data, and drafting or revision of the manuscript. H.-M.H., O.H., and I.R.V.: acquisition, analysis, and interpretation of data. P.I.H.B.: analysis and interpretation of data, and drafting or revision of the manuscript. M.G.: study conception and design, analysis and interpretation of data, and drafting or revision of the manuscript.

ACKNOWLEDGMENTS

The excellent technical support of Sabine Dongard, Anette Langerak, Petra Glitz, and Bernd Fieber is gratefully acknowledged.

This study was funded by the Max-Planck/Fraunhofer interdisciplinary project CryoSystems.

REFERENCES

1. Pegg, D. E. 2007. Principles of cryopreservation. *Methods Mol. Biol.* 368:39–57.
2. Salzmann, C. G., P. G. Radaelli, …, J. L. Finney. 2011. The polymorphism of ice: five unresolved questions. *Phys. Chem. Chem. Phys.* 13:18468–18480.
3. Malenkov, G. 2009. Liquid water and ices: understanding the structure and physical properties. *J. Phys. Condens. Matter.* 21:283101.
4. Loerting, T., K. Winkel, …, D. T. Bowron. 2011. How many amorphous ices are there? *Phys. Chem. Chem. Phys.* 13:8783–8794.
5. Dubochet, J. 2012. Cryo-EM–the first thirty years. *J. Microsc.* 245:221–224.
6. Mazur, P. 1963. Kinetics of water loss from cells at subzero temperatures and the likelihood of intracellular freezing. *J. Gen. Physiol.* 47:347–369.
7. Pegg, D. E. 2010. The relevance of ice crystal formation for the cryopreservation of tissues and organs. *Cryobiology.* 60 (3, Suppl): S36–S44.
8. Lovelock, J. E. 1953. The mechanism of the protective action of glycerol against haemolysis by freezing and thawing. *Biochim. Biophys. Acta.* 11:28–36.
9. Edgar, D. H., and D. A. Gook. 2012. A critical appraisal of cryopreservation (slow cooling versus vitrification) of human oocytes and embryos. *Hum. Reprod. Update.* 18:536–554.
10. Rall, W. F., and G. M. Fahy. 1985. Ice-free cryopreservation of mouse embryos at -196 degrees C by vitrification. *Nature.* 313:573–575.
11. Wowk, B. 2010. Thermodynamic aspects of vitrification. *Cryobiology.* 60:11–22.
12. Fahy, G. M., and B. Wowk. 2015. Principles of cryopreservation by vitrification. *Methods Mol. Biol.* 1257:21–82.
13. Pegg, D. E. 2015. Principles of cryopreservation. *Methods Mol. Biol.* 1257:3–19.
14. Mazur, P. 1984. Freezing of living cells: mechanisms and implications. *Am. J. Physiol.* 247:C125–C142.
15. Dubochet, J., M. Adrian, …, P. Schultz. 1988. Cryo-electron microscopy of vitrified specimens. *Q. Rev. Biophys.* 21:129–228.
16. Hopkins, J. B., R. Badeau, …, R. E. Thorne. 2012. Effect of common cryoprotectants on critical warming rates and ice formation in aqueous solutions. *Cryobiology.* 65:169–178.
17. Seki, S., and P. Mazur. 2012. Ultra-rapid warming yields high survival of mouse oocytes cooled to -196°c in dilutions of a standard vitrification solution. *PLoS One.* 7:e36058.
18. Seki, S., and P. Mazur. 2009. The dominance of warming rate over cooling rate in the survival of mouse oocytes subjected to a vitrification procedure. *Cryobiology.* 59:75–82.
19. Kuleshova, L. L., D. R. MacFarlane, …, J. M. Shaw. 1999. Sugars exert a major influence on the vitrification properties of ethylene glycol-based solutions and have low toxicity to embryos and oocytes. *Cryobiology.* 38:119–130.
20. Bouchet-Marquis, C., V. Starkuviene, and M. Grabenbauer. 2008. Golgi apparatus studied in vitreous sections. *J. Microsc.* 230:308–316.
21. Pedro, P. B., S. E. Zhu, …, M. Kasai. 1997. Effects of hypotonic stress on the survival of mouse oocytes and embryos at various stages. *Cryobiology.* 35:150–158.
22. Gualtieri, R., V. Mollo, …, R. Talevi. 2011. Ultrastructure and intracellular calcium response during activation in vitrified and slow-frozen human oocytes. *Hum. Reprod.* 26:2452–2460.
23. Prentice-Biensch, J. R., J. Singh, …, M. Anzar. 2012. Vitrification of immature bovine cumulus-oocyte complexes: effects of cryoprotectants, the vitrification procedure and warming time on cleavage and embryo development. *Reprod. Biol. Endocrinol.* 10:73.
24. Hochi, S., T. Terao, …, M. Hirao. 2004. Successful vitrification of pronuclear-stage rabbit zygotes by minimum volume cooling procedure. *Theriogenology.* 61:267–275.
25. Coticchio, G., J. J. Bromfield, …, D. F. Albertini. 2009. Vitrification may increase the rate of chromosome misalignment in the metaphase II spindle of human mature oocytes. *Reprod. Biomed. Online.* 19 (*Suppl 3*):29–34.
26. Beier, A. F. J., J. C. Schulz, …, H. Zimmermann. 2011. Effective surface-based cryopreservation of human embryonic stem cells by vitrification. *Cryobiology.* 63:175–185.
27. Iwayama, H., S. Hochi, …, Y. Fukui. 2004. Effects of cryodevice type and donors' sexual maturity on vitrification of minke whale (Balaenoptera bonaerensis) oocytes at germinal vesicle stage. *Zygote.* 12:333–338.

28. Al-Amoudi, A., L. P. O. Norlen, and J. Dubochet. 2004. Cryo-electron microscopy of vitreous sections of native biological cells and tissues. *J. Struct. Biol.* 148:131–135.

29. Tirtaatmadja, V., D. E. Dunstan, and D. V. Boger. 2001. Rheology of dextran solutions. *J. Nonnewton. Fluid Mech.* 97:295–301.

30. Cha, S., S. H. Kim, and D. Kim. 2010. Viscosity of sucrose aqueous solutions measured by fluorescence correlation spectroscopy. *J. Korean Phys. Soc.* 56:1315–1318.

31. Zamir, T., and A. Khan. 2005. Study of ion-solvent interactions of lithium bromide in DMSO, H2O and DMSO-H2O mixtures at 25°C. *J. Chem. Soc. Pak.* 27:130–136.

32. Hayduk, W., and V. K. Malik. 1971. Density, viscosity, and carbon dioxide solubility and diffusivity in aqueous ethylene glycol solutions. *J. Chem. Eng. Data.* 16:143–146.

33. Herskovits, T. T., and T. M. Kelly. 1973. Viscosity studies of aqueous solutions of alcohols, ureas, and amides. *J. Phys. Chem.* 77:381–388.

34. Leunissen, J. L., and H. Yi. 2009. Self-pressurized rapid freezing (SPRF): a novel cryofixation method for specimen preparation in electron microscopy. *J. Microsc.* 235:25–35.

35. Han, H. M., J. Huebinger, and M. Grabenbauer. 2012. Self-pressurized rapid freezing (SPRF) as a simple fixation method for cryo-electron microscopy of vitreous sections. *J. Struct. Biol.* 178:84–87.

36. Grabenbauer, M., H.-M. Han, and J. Huebinger. 2014. Cryo-fixation by self-pressurized rapid freezing. *Methods Mol. Biol.* 1117:173–191.

37. Sun, J., and H. Li. 2010. How to operate a cryo-electron microscope. *Methods Enzymol.* 481:231–249.

38. Kremer, J. R., D. N. Mastronarde, and J. R. McIntosh. 1996. Computer visualization of three-dimensional image data using IMOD. *J. Struct. Biol.* 116:71–76.

39. Mastronarde, D. N. 1997. Dual-axis tomography: an approach with alignment methods that preserve resolution. *J. Struct. Biol.* 120: 343–352.

40. Pettersen, E. F., T. D. Goddard, …, T. E. Ferrin. 2004. UCSF Chimera–a visualization system for exploratory research and analysis. *J. Comput. Chem.* 25:1605–1612.

41. Vajta, G., P. Holm, …, H. Callesen. 1998. Open pulled straw (OPS) vitrification: a new way to reduce cryoinjuries of bovine ova and embryos. *Mol. Reprod. Dev.* 51:53–58.

42. Arav, A. 2014. Cryopreservation of oocytes and embryos. *Theriogenology.* 81:96–102.

43. Paredes, E., and P. Mazur. 2013. The survival of mouse oocytes shows little or no correlation with the vitrification or freezing of the external medium, but the ability of the medium to vitrify is affected by its solute concentration and by the cooling rate. *Cryobiology.* 67:386–390.

44. Turnbull, D. 1969. Under what conditions can a glass be formed? *Contemp. Phys.* 10:473–488.

45. Yavin, S., and A. Arav. 2007. Measurement of essential physical properties of vitrification solutions. *Theriogenology.* 67:81–89.

46. Dubochet, J. 2007. The physics of rapid cooling and its implications for cryoimmobilization of cells. *Methods Cell Biol.* 79:7–21.

47. Spindler, R., W. F. Wolkers, and B. Glasmacher. 2011. Dimethyl sulfoxide and ethylene glycol promote membrane phase change during cryopreservation. *Cryo Lett.* 32:148–157.

48. Akhoondi, M., H. Oldenhof, …, W. F. Wolkers. 2011. Membrane hydraulic permeability changes during cooling of mammalian cells. *Biochim. Biophys. Acta.* 1808:642–648.

49. Walters, K. R., Jr., A. S. Serianni, …, J. G. Duman. 2009. A nonprotein thermal hysteresis-producing xylomannan antifreeze in the freeze-tolerant Alaskan beetle Upis ceramboides. *Proc. Natl. Acad. Sci. USA.* 106:20210–20215.

50. Gibson, M. I. 2010. Slowing the growth of ice with synthetic macromolecules: beyond antifreeze(glyco) proteins. *Polym. Chem.* 1:1141.

51. Balcerzak, A. K., S. S. Ferreira, …, R. N. Ben. 2012. Structurally diverse disaccharide analogs of antifreeze glycoproteins and their ability to inhibit ice recrystallization. *Bioorg. Med. Chem. Lett.* 22:1719–1721.

52. Venketesh, S., and C. Dayananda. 2008. Properties, potentials, and prospects of antifreeze proteins. *Crit. Rev. Biotechnol.* 28:57–82.